

## The Impact of Selected Air Pollutants on Spatial PEMFC Performance

Tatyana Reshетенko, Jean St-Pierre

Hawaii Natural Energy Institute,  
University of Hawai'i, Honolulu, HI 96822

Proton exchange membrane fuel cells (PEMFCs) continue to be the subject of intensive research and development efforts because they are considered as a promising alternative and clean energy sources. Since most fuel cells operate with air as an oxidant, cathode exposure to air contaminants ( $\text{SO}_2$ ,  $\text{H}_2\text{S}$ ,  $\text{NH}_3$ ,  $\text{NO}_x$ , and some organic compounds) can cause damage and a significant performance loss (1, 2). From an inventory of 260 common air pollutants, seven contaminants were chosen using a 2 tiered down selection process for detailed studies (3). These seven pollutants are organic compounds: acetylene ( $\text{C}_2\text{H}_2$ ), propene ( $\text{C}_3\text{H}_6$ ), methyl methacrylate (MMA,  $\text{CH}_2\text{C}(\text{CH}_3)\text{COOCH}_3$ ), 2-propanol ( $(\text{CH}_3)_2\text{CHOH}$ ), bromomethane ( $\text{CH}_3\text{Br}$ ), naphthalene ( $\text{C}_{10}\text{H}_8$ ), and acetonitrile ( $\text{CH}_3\text{CN}$ ), which are commonly used as solvents, synthesis precursors, fuels, cleaning agents, or for pest control. Detailed information about the current distribution is crucial and beneficial for understanding the poisoning process and to improve the PEMFC environmental adaptability and durability. In this work, the spatial fuel cell performance under separate exposure of  $\text{C}_3\text{H}_6$ ,  $\text{C}_2\text{H}_2$ ,  $\text{CH}_3\text{Br}$  and MMA was studied with a segmented cell system.

A segmented cell and data acquisition system was used (4) with a commercially available  $100\text{ cm}^2$  membrane/electrode assembly (MEA). Each electrode contained a Pt/C catalyst with a loading of  $0.4\text{ mg}_{\text{Pt}}\text{ cm}^{-2}$ . A segmented SGL 25BC gas diffusion layer (GDL, 10 segments of  $7.6\text{ cm}^2$ ) and a Teflon gasket were used at the cathode whereas a single GDL piece was applied at the anode. The MEA was operated at  $1.0\text{ A cm}^{-2}$ ,  $80^\circ\text{C}$ ,  $48.3\text{ kPa}_g$  back pressure and 100/50% relative humidity for the anode and cathode respectively. The dry contaminant was injected into the humidified cathode air stream. The contamination proceeded until the cell voltage reached a steady value. Subsequently, the contaminant injection was stopped to evaluate the cell recovery ability in air.

Fig. 1 shows the voltage response and current density for each segment normalized with its initial performance vs. experiment time. For the first 17 h, the cell was operated with pure air resulting in a cell voltage of 0.662 V. The injection of 300 ppm  $\text{C}_2\text{H}_2$  significantly decreased the voltage during a transition period that lasted 40 min eventually reaching a steady state of 0.074 V. The voltage decrease was accompanied by a significant change in the current density distribution especially during the transition period. At steady state, the inlet segments 1-4 showed a decrease in current due to  $\text{C}_2\text{H}_2$  impact. By contrast, downstream segments demonstrated an increase in current despite the presence of the contaminant.

Fig. 2 shows spatial electrochemical impedance spectroscopy (EIS) data for segments 1, 4, 7, and 10, recorded during various experiment phases. A significant increase in impedance response for all segments was observed after 1 h of  $\text{C}_2\text{H}_2$  exposure. EIS curves for segments 1-9 demonstrated a pseudo-inductive loop at

low frequencies which might be attributed to  $\text{C}_2\text{H}_2$  chemisorption and its subsequent slow conversion. Segment 10 showed a negative impedance loop which might be attributed to  $\text{O}_2$  depletion in addition to poisoning. Detailed analysis of the current density distribution and its correlation with EIS data will be presented and discussed for other selected contaminants.

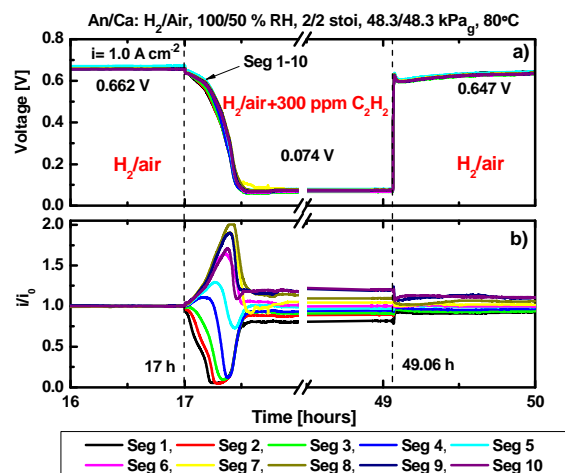


Fig. 1. Voltage (a) and current density for each segment normalized with its initial performance (b) vs. time.

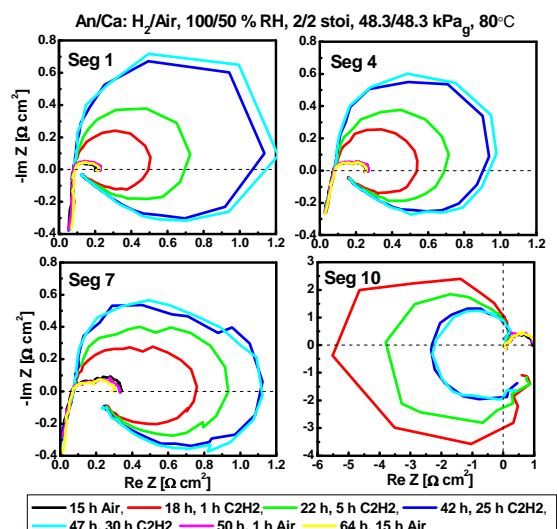


Fig. 2. Electrochemical impedance spectra for segments 1, 4, 7, 10 during the different phases of exposure to 300 ppm  $\text{C}_2\text{H}_2$ .

### ACKNOWLEDGEMENTS

We gratefully acknowledge DOE funding (DE-EE0000467). Authors are grateful to the Hawaiian Electric Company for their ongoing support to the operations of the Hawaii Sustainable Energy Research Facility.

### REFERENCES

1. X. Cheng, Z. Shi, N. Glass, L. Zhang, D. Song, Z. Liu, H. Wang, J. Shen, *J. Power Sources*, **165**, 739 (2007).
2. Y. Zhai, J. St-Pierre, M. Angelo, *ECS Trans.*, **50** (2), 635 (2012).
3. J. St-Pierre, M.S. Angelo, Y. Zhai, *ECS Trans.*, **41**(1), 279 (2011).
4. T.V. Reshетенko, G. Bender, K. Bethune, R. Rocheleau, *Electrochim. Acta*, **56**, 8700 (2011).